New Approach to the Formation Mechanism of AgCl Nanoparticles in a Reverse Micelle System

Tadao Sugimoto* and Ken'ichi Kimijima

Institute of Multidisciplinary Research for Advanced Materials, Tohoku University, Katahira 2-1-1, Aoba-ku, Sendai 980-8577, Japan

Received: May 14, 2003; In Final Form: July 19, 2003

The formation mechanism of uniform AgCl nanoparticles in a reverse micelle (RM) system of polyoxyethylene (6) nonylphenyl ether/water/cyclohexane has been investigated through a new approach that uses a double jet technique, in which $AgNO_3$ and KCl in RM solutions were continuously introduced at the same time. The final particle number was proportional to the feed rate of the reactants, in the same way as in the conventional double jet process in an aqueous gelatin solution (AGS) system. The experimental results in both systems were in excellent agreement with the theoretical prediction that was based on a diffusion-controlled growth model, where the reverse micelles that contained Ag ions in the RM system primarily carried only one Ag ion, and thus they were regarded as a type of Ag-ion complex that diffuses in the organic medium to be reacted with AgCl particles that have been stabilized by the surfactant. Thus, the dramatic reduction of particle size in the RM system was due to the extremely small growth rate of the nuclei, which was caused by the very low solubility of the solid in the RM solution, in terms of the concentration of the micellar Ag-ion complex in the organic medium and the small diffusivity of the bulky Ag-ion complex, in contrast to the conventional explanation, mainly in terms of the limited dimensions of the reverse micelles as nanotemplates. The exceedingly low substantial solubility of solid seems to be, at least, one of the main reasons for the formation of ultrafine nanoparticles in general RM systems.

Introduction

Considerably uniform ultrafine particles can readily be obtained in reverse micelle (RM) systems; therefore, the synthesis of nanoparticles in such systems has widely been attempted for pure metals,[1−3] metal oxides,[4,5] metal sulfides,[6,7] silver halides,[8−14] polymers,[15,16] etc. Because of the characteristic features of the system, the mechanism for the formation of nanoparticles in such a system has usually been explained on the basis of the reaction in the individual water pools of the reverse micelles. Therefore, it seems to be generally accepted that the particle size is mainly determined by the size of the water pools as a reaction field, bound by the colloidal assemblies of surfactant molecules as a template that confines each reaction field.[17,18] On the other hand, it is well-known that reverse micelles rapidly repeat the association and dissociation processes at a rate on the order of 10^6-10^8 mol^{-1} dm^3 s^{-1}.[19] Actually, the reaction between Ag^+ and Cl^- ions in a RM system was completed within ca. 60 ms, as revealed from the stopped-flow measurement.[9,10] This time scale is comparable to the reaction time for Ag^+ and Cl^- ions in a plain aqueous solution.[20,21] In addition, the dimensions of the product particles are often much greater than the size of a water pool.[17] In view of these facts, the concept of confined nanoreactors, or nanotemplates, separated by an oil medium seems to involve an essential inconsistency with the dynamic and fluid nature of reverse micelles.

The objective of the present study is to give essential insight into the fundamental mechanism of the particle formation of AgCl in a RM system, using a specific mixing method with continuous and simultaneous feed of reactants, the so-called double jet technique, by changing the feed rate of the simultaneous introduction of Ag and Cl ions. The results are discussed in comparison with the corresponding conventional aqueous gelatin solution (AGS) system. The final conclusions may apply to the underlying mechanism of particle formation in general RM systems.

Experimental Section

Chemicals. Polyoxyethylene (6) nonylphenyl ether (NP-6), which was kindly furnished by Lion Co., Ltd., was purified by washing repeatedly with butanol, according to the procedure in the literature,[22] followed by drying at 65 °C in a vacuum. Cyclohexane (Wako Pure Chemical Industries, Ltd.) was dehydrated with a type 3A molecular sieve and percolated through a membrane filter with a pore size of 0.2 μm (Toyo Roshi Kaisha, Ltd.). $AgNO_3$ and KCl of special reagent grade were used as received (Wako Pure Chemical Industries, Ltd.). Water was doubly distilled.

Preparation of AgCl Particles in a Reverse Micelle (RM) System. Aqueous solutions of 1.00×10^{-2} mol/dm^3 $AgNO_3$, 1.20×10^{-2} mol/dm^3 KCl, and 1.00×10^{-3} mol/dm^3 KCl were prepared beforehand. Each of these salt solutions was admixed with 0.10 mol/dm^3 NP-6 in cyclohexane, to prepare three types of RM solutions. Here, the Rw value ($Rw \equiv [H_2O]/[NP\text{-}6]$) was fixed at 3. In the standard procedure, 6 cm^3 of the $AgNO_3$ RM solution and the same volume of the KCl (1.20×10^{-2} mol/dm^3 in water) RM solution were simultaneously added to 20 cm^3 of the other KCl (1.00×10^{-3} mol/dm^3 in water) RM solution at a constant rate of 0.20 cm^3/min for 30 min at 30 °C under magnetic agitation, using a constant flow rate pump (Watson Marlow Ltd., model 101U/R). Thus, the excess

* Author to whom correspondence should be addressed. E-mail: sugimoto@tagen.tohoku.ac.jp.

10.1021/jp035329w CCC: $25.00
Published on Web 09/09/2003

concentration of Cl^- ions in the water phase was nominally kept constant at 1.00×10^{-3} mol/dm^3 during the mixing process. Immediately after the completion of the simultaneous addition of the RM solutions of $AgNO_3$ and KCl, 0.06 cm^3 of a 10^{-2} mol/dm^3 4-hydoroxy-6-methyl-1,3,3a,7-tetraazaindene (TAI) aqueous solution was added, to halt any further processes, such as Ostwald ripening. A volume (13 cm^3) of methanol that contained 10^{-3} mol/dm^3 TAI then was added, to cause phase separation between cyclohexane and a mixed solvent of methanol and water, the latter of which was used to keep the AgCl particles well dispersed. The AgCl particles were collected by centrifugation (6000 rpm for 45 min) and dispersed in distilled water, to be used as a transmission electron microscopy (TEM) sample. All operations were conducted in photochemically inactive red light.

Preparation of AgCl Particles in an Aqueous Gelatin Solution (AGS) System. We also prepared uniform AgCl particles using the conventional double jet method, in which aqueous solutions of $AgNO_3$ and KCl were concurrently added to a KCl solution that contained gelatin at a constant rate, to compare the data with those of the RM system. The standard procedure is as follows.

A volume (30 cm^3) of 1.00×10^{-2} mol/dm^3 $AgNO_3$ and the same volume of 1.20×10^{-2} mol/dm^3 KCl were added simultaneously to 100 cm^3 of 1.00×10^{-3} mol/dm^3 KCl solution that contained 2.0 w/v % gelatin (P-459, from Miyagi Chemical Industrial Co., Ltd.), using a constant flow rate pump under magnetic agitation for 30 min (1.0 cm^3/min) at 30 °C. The pH of the gelatin solution with 1.00×10^{-3} mol/dm^3 KCl was 5.77. Immediately after the double jet process, 1 cm^3 of a 0.04 mol/dm^3 TAI aqueous solution was added to stop the reaction. The particles were then washed twice with doubly distilled water by centrifugation (6000 rpm for 45 min) and observed by TEM. All experiments were performed in the red light.

Measurement of the Mean Size of AgCl Particles. The mean size of AgCl particles was obtained by computer analysis on their TEM images.

Adsorption Isotherm of NP-6 to AgCl Particles. The adsorption isotherm was obtained by changing the concentration of NP-6 in 50 cm^3 of an aqueous suspension of a AgCl powder (1 g). The AgCl powder was previously prepared by mixing 3.0 mol/dm^3 $AgNO_3$ and the same volume of 3.2 mol/dm^3 KCl that contained 2 w/v% gelatin at 25 °C. Gelatin was decomposed using an enzyme (trypsin, from Wako Pure Chemical Industries, Ltd.), and then the precipitate was repeatedly washed with doubly distilled water by centrifugation, followed by drying. The specific surface area of the AgCl powder was measured by the Brunauer−Emmett−Teller (BET) method (Micromeritics Instruments, model ASAP 2010). After aging for 6 h at 30 °C under magnetic agitation and centrifugal separation (3000 rpm for 30 min), the supernatant concentrations of NP-6 were measured by UV spectroscopy at a wavelength of $\lambda = 224.4$ nm to determine the adsorbed amount of NP-6.

Measurement of the Mean Size of a Reverse Micelle. The mean size of a reverse micelle, without the reactants and product, was measured at room temperature by small-angle X-ray scattering (SAXS). The mean diameter of the reverse micelles was calculated by the Guinier method from the SAXS profile, applying the assumption that their shape was spherical. The thus-obtained mean size was used for the calculation of the number density of the reverse micelles and their diffusivity by the Stokes−Einstein equation.

Measurement of the Viscosities of the RM and AGS Systems. The viscosity of the RM solution of the standard composition, but without $AgNO_3$ and KCl, and that of the gelatin solution, which contained 2.0 w/v% gelatin and 1.00×10^{-3} mol/dm^3 KCl, were measured with an Ubbelohde viscometer at 30 °C. These data were used for the calculation of the diffusivities of the reverse micelles in the RM system and the Ag-ion complexes in the AGS system.

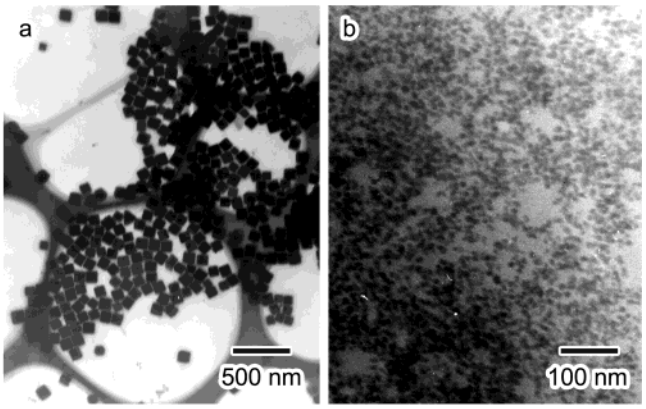

Figure 1. TEM photos of AgCl particles prepared under the standard conditions: (a) aqueous gelatin solution (AGS) system, (b) reverse micelle (RM) system.

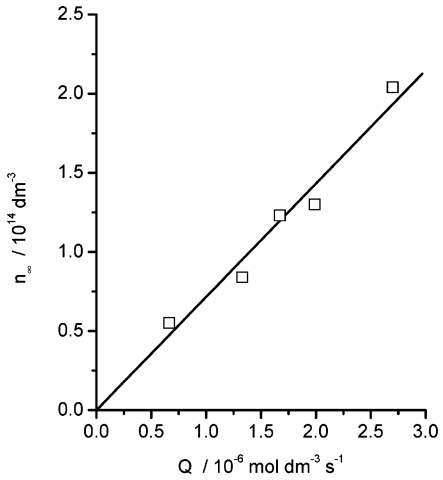

Figure 2. Final number density (n_∞) of the AgCl particles, as a function of the feed rate (Q) of $AgNO_3$, in the double jet process in the AGS system at 30 °C.

Results and Discussion

Dependence of the Particle Number Density on the Feed Rate of Solute. Figure 1a shows a TEM image of AgCl particles that have been prepared by the conventional double jet method in an AGS system under the standard conditions (see Experimental Section). The mean edge length was 85.8 nm, and the coefficient of variation of the size distribution was 13.9%. On the other hand, Figure 1b shows a TEM image of the AgCl particles that have been prepared using a similar mixing procedure in a RM system under the standard conditions (see Experimental Section). The particle shape was spheroidal, in contrast to those obtained in the aqueous gelatin solution. The mean diameter was 10.0 nm, and the coefficient of variation of the size distribution was 18.3%.

Figure 2 shows the final number density (n_∞) as a function of the feed rate (Q) of $AgNO_3$ in the AGS system at 30 °C. Here, n_∞ and Q were defined as the final particle number and the molal feed rate, respectively, per unit volume of the gelatin solution initially in the reaction vessel prior to the addition of

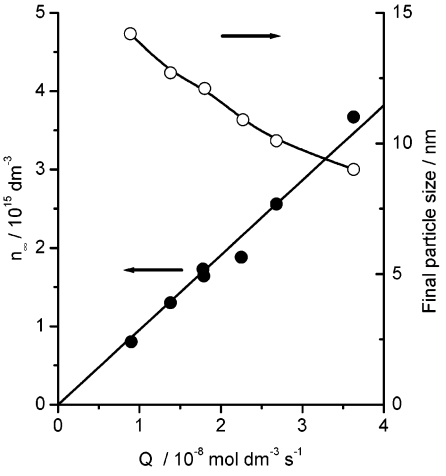

Figure 3. (●) Final number density (n_∞) and (○) final particle size, each as a function of the feed rate (Q) of $AgNO_3$, in the double jet process in the RM system. The amount of Ag ions added was fixed at 1.08×10^{-6} mol.

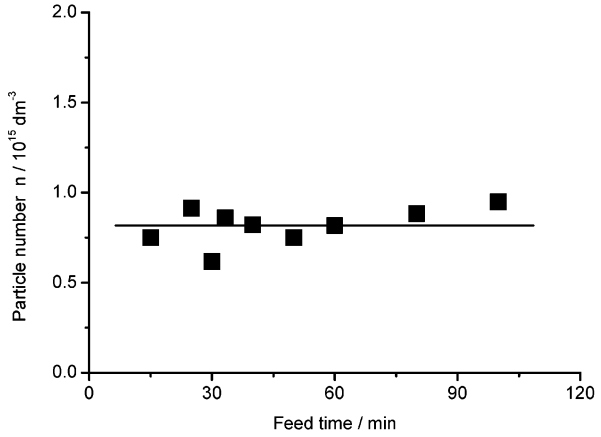

Figure 4. Relationship between the number density of the AgCl particles (n) and the reaction time for the double jet process in the RM system. The addition rate of $AgNO_3$ was 9.00×10^{-9} mol dm^{-3} s^{-1}.

the reactants. The figure clearly demonstrates that n_∞ is proportional to Q, in agreement with the results of Leubner.[23] Similar proportionality was also observed for n_∞ vs Q in the RM system, as shown in Figure 3. The definition of n_∞ is the same as that in the AGS system, i.e., the final number density per unit volume of the RM solution initially in the reaction vessel. Corresponding final particle sizes are also shown in Figure 3, where the added amount of Ag ions was fixed at 1.08×10^{-6} mol. Also, as shown in Figure 4, the number density (n) of AgCl particle was maintained constant against the feed time of the RM solution of $AgNO_3$ at the standard feed rate of 9.00×10^{-9} mol dm^{-3} s^{-1}, where the data were taken individually for different runs. This observation means that the AgCl particles are grown by the continuous feeding of the solute without renucleation after a very short time for the initial nucleation. This is the reason considerably uniform particles were obtained. Exactly the same trend was observed in the conventional AGS system, as well for the formation of uniform AgCl particles. The mean particle size after the mixing process for 60 min in this RM system was 12.5 nm: much greater than the estimated size of a water pool of a reverse micelle (1.51 nm), which is equivalent to a volume that is 567 times greater than that of the water pool of a reverse micelle. This observation indicates that the final particle size is not confined to the dimensions of the water pools. This is also supported by the

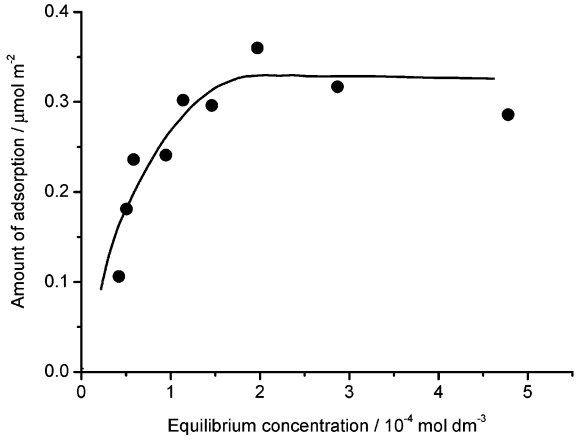

Figure 5. Adsorption isotherm of NP-6 onto the surfaces of AgCl particles in an aqueous solution of NP-6 at 30 °C.

plot of constant particle number density (n) against feed time in Figure 4, instead of its proportional increase, as would be observed if the particle size were limited by the dimensions of a water pool. Moreover, there was no sign of the intermicellar coagulation of the AgCl nuclei, which was supposed by Sato et al.[24] as the main growth process for silver halide particles such as AgBr and AgI in RM systems, because the particle number was maintained constant with feed time in Figure 4. All these results may suggest that the nucleation and growth processes of the AgCl particles in the RM system are governed by almost the same mechanism as that in the AGS system.

In the double jet process of a conventional AGS system, the nucleation of silver halide particles occurs instantaneously in a limited zone of the gelatin solution in the reaction vessel, into which the reactant solutions of Ag ions and halide ions are introduced. The generated nascent nuclei are constantly dispersed into the entire volume of the gelatin solution via agitation. Initially, they are all dissolved until the concentration of the solute reaches the solubility level of the solid. After the solubility level for the relatively large nuclei has been attained, these nuclei start to grow at the expense of the smaller nuclei, which continue to be dissolved. When the relatively large nuclei to be grown (stable nuclei) have accumulated to a certain number density, the increase in the number density of the stable nuclei terminates, because the concentration level of the solute becomes sufficiently low to reach the balance of the total dissolution of all nascent nuclei and the growth of the preformed stable nuclei. This moment corresponds to the end of the nucleation stage for the stable nuclei. The stable nuclei then continue to grow without changing their number, via the steady dissolution of the nascent nuclei constantly generated. This stage corresponds to the growth period of the stable nuclei in this system. In short, silver halide particles are generated and grown by a type of dynamic Ostwald ripening during the mixing process in the conventional AGS system.[21,25,26] Because the exchange of solute among reverse micelles in a RM system is so fast, with a second-order rate constant of 10^6-10^8 mol^{-1} dm^3 s^{-1},[19] there is no doubt that a similar process also proceeds in the RM system in the present study.

Effect of Adsorption of NP-6 onto AgCl Particles. Figure 5 shows the adsorption isotherm of NP-6 onto a AgCl powder (BET surface area of 1.17 m^2/g) in an aqueous solution at 30 °C. The adsorption of NP-6 reached the saturation point at ca. 2×10^{-4} mol/dm^3, ~4 times greater than its critical micelle concentration (CMC), ca. 5.0×10^{-5} mol/dm^3,[27] which suggests additional adsorption of NP-6 micelles above the CMC. However, the saturation adsorption level (~0.33 μmol/m^2) was

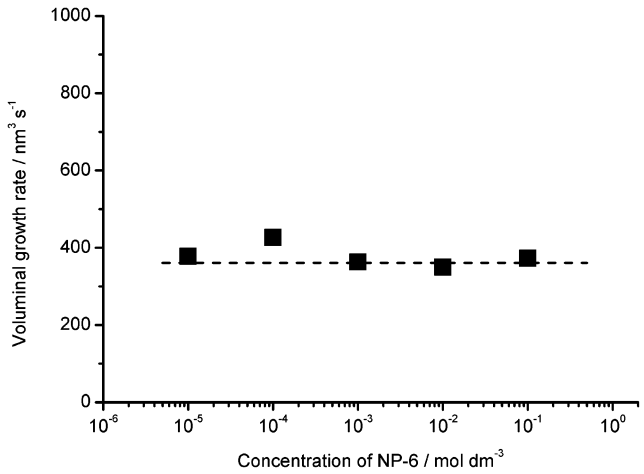

Figure 6. Dependence of the voluminal growth rate on the concentration of NP-6 in its aqueous gelatin solution at 30 °C. Dotted line represents the voluminal growth rate with [NP-6] = 0 at 30 °C.

extremely low, in comparison to typical adsorption isotherms (e.g., the adsorption of sodium oleate onto anatase TiO_2 particles, used as a shape controller of the latter, reaching ca. 20 μmol/m^2).[28] The coagulation among the AgCl particles in the RM system was not observed, as evident from the result in Figure 4; therefore, the AgCl particles were likely to be protected in the cages of the reverse micelles of NP-6, rather than by its direct adsorption. However, even if the adsorption of NP-6 is very weak, it does not necessarily mean that the adsorption of NP-6 has no influence on the growth of AgCl particles. To clarify this point, the effect of NP-6 on the particle growth was examined by adding NP-6 to the gelatin solution of the AGS system, varying its concentration from zero even to 0.10 mol/dm^3 (ca. 500 times greater than the concentration of NP-6 necessary for the saturation adsorption). As shown in Figure 6, NP-6 in the gelatin solution had no influence on the growth of AgCl particles. The AgCl particles were all in the form of sharp-edged cubes, irrespective of the concentration of NP-6. Here, note that gelatin is substantially adsorbed onto silver halides and protects the growing particles,[29] but the adsorbed gelatin does not inhibit the growth of the particles at all. This observation is obvious from the fact that AgCl[30] and AgBr[31] particles in a gelatin solution can grow via the diffusion-controlled mechanism in which the surface reaction process is not the rate-limiting step. In addition, the cubic shape is usual for AgCl, even in the absence of gelatin. Because even gelatin does not have any adverse effect on the growth of AgCl particles, one may conclude that NP-6, as a much weaker adsorbate, has no influence on the growth of particles in the RM system.

The adsorption of NP-6 is unlikely to affect the morphology of the AgCl particles; therefore, the formation of the spherical particle in the RM system may be due to the thermodynamic requirement for minimizing the high specific surface energy of the ultrafine AgCl particles by reducing the surface chemical potential of the {111} and {110} faces.[21,32]

Analysis on the Basis of the Nucleation Theory. If the supply rate of solute is independent of the growth rate of the generated nuclei in a monodispersed particle system, the following general formula applies:[21,33]

$$n_\infty = \left(\frac{V_m}{\dot{v}}\right)Q \qquad (1)$$

where n_∞ is the final number density of the product particles

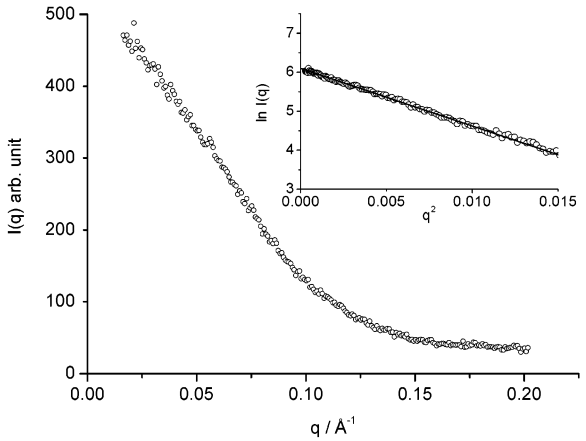

Figure 7. Small-angle X-ray scattering (SAXS) profiles for the RM system (0.1 mol/dm^3 NP-6 in cyclohexane, Rw = 3), where q is the scattering vector. Inset shows the Guinier plot.

per initial unit volume of the solution in the reactor, V_m the molar volume of the solid, Q the supply rate of the solute per initial unit volume of the solution in the reactor, and $\dot{v}$ the growth rate in volume of the stable nuclei at the end of the nucleation stage. This equation covers not only the usual formation process of monodispersed particles through spontaneous nucleation and the subsequent growth, but also the formation process through the aforementioned dynamic Ostwald ripening process. Moreover, the equation is valid irrespective of the growth mechanism, such as the diffusion-controlled or the reaction-controlled growth mode. Specifically, Sugimoto[25] derived theoretically the following formula of n_∞ for a system of the dynamic Ostwald ripening in the diffusion-controlled growth mode:

$$n_\infty = \left(\frac{1.567}{\sigma}\right)\left(\frac{QRT}{8\pi D V_m C_\infty}\right) \qquad (2)$$

where σ is the specific surface energy of the solid, R the gas constant, T the absolute temperature, D the diffusion coefficient of the solute, and C_∞ the solubility of the bulk solid. The variables n_∞ and Q have the same meanings as in eq 1. This theoretical formula was applied to the double jet procedure for the formation of monodispersed AgBr particles in a diffusion-controlled dynamic Ostwald ripening process and verified from the analysis of the experimental results.

From eqs 1 and 2, the parameter $\dot{v}$ in a diffusion-controlled dynamic Ostwald ripening system may be written as

$$\dot{v} = \left(\frac{\sigma}{1.567}\right)\left(\frac{8\pi D V_m^2 C_\infty}{RT}\right) \qquad (3)$$

AgCl particles are well-known to grow in a diffusion-controlled mode;[30] therefore, eq 3 may be applicable, at least, to the double jet procedure in the AGS system for AgCl particles.

Here, it seems worthwhile to examine the characteristic features of the RM system in the present study. Figure 7 shows a SAXS profile of the RM system of the standard composition, but without salts such as $AgNO_3$ and KCl. The Guinier plot of the SAXS data in the same figure shows that the mean diameter of the reverse micelles was 3.26 nm. Assuming that shape of the reverse micelle is that of a compact sphere, consisting of NP-6 and H_2O in a molar ratio of 1:3, the average numbers of the molecules of NP-6 and H_2O are calculated to be 20.2 and 60.7 in a reverse micelle, using a value of 0.997 g/cm^3 for the density of NP-6. Hence, the average numbers of Ag^+ and Cl^- ions in each RM reactant solution are calculated to be 1.09 ×

TABLE 1: Average Numbers of the Chemical Species in a Reverse Micelle in the RM System[a]

species	average number per micelle
H_2O	60.7
NP-6	20.2
Ag^+ in $AgNO_3$ RM solution	1.09×10^{-2}
Cl^- in KCl RM solution	1.31×10^{-2}
Cl^- in RM solution in reaction	1.09×10^{-3}
$AgCl_n^{(n-1)-}$ in RM solution in reaction	9.0×10^{-7}
AgCl particles in RM solution after the reaction	1.7×10^{-7}

[a] Rw = 3; [NP-6] = 0.1 mol/dm^3 in cyclohexane.

10^{-2} and 1.31×10^{-2} from $[AgNO_3]/[H_2O] = 1.80 \times 10^{-4}$ and $[KCl]/[H_2O] = 2.16 \times 10^{-4}$. In other words, the reverse micelles, which actually contain Ag^+ or Cl^- ions, primarily carry only one ion, and the fractions of such reverse micelles, relative to the total number of reverse micelles in the respective micellar solutions, are only 1.09×10^{-2} and 1.31×10^{-2}, respectively. When the mixing process starts, AgCl nuclei become incorporated in some reverse micelles in the reaction vessel, and the total concentration of the silver complexes must be kept at the solubility level of the nuclei of the arithmetic mean size,[21] somewhat higher than that of the bulk solid. If the total concentration of the silver complexes in the water pools of the reverse micelles at 30 °C is approximated by the solubility of AgCl bulk solid in an aqueous solution, one obtains a value of 8.2×10^{-7} mol/dm^3 from all concentrations of each silver complex calculated with the solubility product of AgCl, stability constants of each complex, and enthalpy changes with their formation.[34] As a result, the fraction of the reverse micelles that carry a silver complex in the reaction vessel is estimated to be 9.0×10^{-7}, and, thus, the number of silver complexes in such a micelle is literally only one. Also, the fraction of the reverse micelles that contain a AgCl particle in the final stage of the mixing process is estimated to be 1.7×10^{-7} from the final size of the product particles (10.0 nm). Because the zero point of charge of AgCl is ca. 5.2 in pCl (pCl $\equiv -\log [Cl^-]$),[35] the surfaces of the AgCl particles may be, more or less, covered with Cl^- ions in the presence of 10^{-3} mol/dm^3 Cl^- ions in water. The average numbers of the chemical species in a reverse micelle are summarized in Table 1. The concentrations of each $AgCl_n^{(n-1)-}$ complex in an aqueous solution in equilibrium with AgCl bulk solid at 30 °C are listed with the related constants in Table 2. The major Ag ion species in the RM system with AgCl particles are the neutral AgCl complex and Ag^+ cations, as found in this table.

From this overview, one may regard a reverse micelle that carries a Ag ion or its chloride complex as a type of bulky Ag-ion complex in the cyclohexane medium. When a micellar silver complex encounters a reverse micelle that contains a AgCl particle, the AgCl molecule or Ag^+ ion involved in the micellar silver complex may deposit onto the AgCl particle directly or after reaction with Cl^- ions that are adsorbed on the AgCl particle. In the meantime, the nascent nuclei that is constantly generated may furnish new micellar silver complexes by their own dissolution, to compensate for the Ag ion used for the growth of the stable AgCl particles. Thus, it seems that one may treat the growth of AgCl particles in the RM system essentially in the same way as in the conventional AGS system, irrespective of the differences in the species of the medium and in the size of the silver complexes. As a consequence, the solubility of AgCl bulk solid in the RM system may be defined as the concentration of the micellar silver complexes in equilibrium with AgCl bulk crystals. If the solubility of AgCl bulk solid in an aqueous solution (C_∞^w) can be used as the solubility in the water phase of a RM system, the solubility of AgCl bulk solid in the RM system, C_∞, may be written as

$$C_\infty = C_\infty^w \frac{V_w}{V_w + V_O} \tag{4}$$

where V_w and V_O are the total volume of water and oil (cyclohexane) in the RM solution in the reaction vessel. Using the values $C_\infty^w = 8.22 \times 10^{-7}$ mol/dm^3 and $V_w/(V_w + V_O) = 5.4 \times 10^{-3}$, one obtains $C_\infty = 4.44 \times 10^{-9}$ mol/dm^3. If the growth of the AgCl particles in a RM system is controlled by the diffusion of the micellar silver complex, eqs 1−3 may also be applicable to the RM system. In this case, C_∞ in eqs 2 and 3 is given by eq 4.

The diffusion coefficient (D) for the micellar silver complex may be given by the Stokes−Einstein equation:

$$D = \frac{kT}{6\pi\eta r} \tag{5}$$

where k is the Boltzmann constant, T the absolute temperature, η the viscosity of the medium, and r the radius of a reverse micelle. In the present RM system, $r = 1.63$ nm (from SAXS) and $\eta = 0.99$ mPa s (from the measurement of the viscosity of the RM system), so that $D = 1.38 \times 10^{-10}$ m^2/s at 30 °C.

Correspondingly, C_∞ and D values in the AGS system may be given from the following procedure. Because the parameter C_∞ in this system is the total of the concentrations of $AgCl_n^{(n-1)-}$ complexes ($n \geq 0$) and silver−gelatin complexes in equilibrium with AgCl bulk solid, the Ag^+ ion linked to a side-chain group of gelatin is assumed to be promptly released in the form of $AgCl_n^{(n-1)-}$ complexes, in response to the change of the ambient Ag^+ concentration.[33] The concentrations of each $AgCl_n^{(n-1)-}$ complex in equilibrium with AgCl bulk solid and their total are available in Table 2. The concentrations of each silver−gelatin complex at pH 5.77 were calculated from the contents of the effective amino acid residues in gelatin,[36] the stability constants of their silver complexes (β) at 30 °C,[37] and their acidic dissociation constants (pK_a) at 25 °C,[38] according to the method of Harding.[39] The results are summarized in Table 3.

TABLE 2: Cumulative Stability Constants (β), Enthalpy Change in Formation (ΔH), and Equilibrium Concentration of Silver Chloride Complexes ($[AgCl_n^{(n-1)-}]$) in an Aqueous Suspension of AgCl at 30 °C

$AgCl_n^{(n-1)-}$	β,[a] 25 °C	ΔH (kJ/mol)	β,[a] 30 °C	$[AgCl_n^{(n-1)-}]$, at 30 °C (mol/dm^3)	
Ag^+				2.73×10^{-7}	$[Cl^-] = 1.00 \times 10^{-3}$ mol/dm^3
AgCl	$10^{3.3}$	−11	$10^{3.27}$	5.05×10^{-7}	$K_{sp} = 2.73 \times 10^{-10}$
$AgCl_2^-$	$10^{5.25}$	−16	$10^{5.20}$	4.35×10^{-8}	
$AgCl_3^{2-}$	$10^{5.7}$	−24	$10^{5.63}$	1.16×10^{-10}	$\sum_{n=0}[AgCl_n^{(n-1)-}] = 8.22 \times 10^{-7}$ mol/dm^3
$AgCl_4^{3-}$	$10^{5.4}$	−58	$10^{5.23}$	4.66×10^{-14}	

[a] $\beta = [AgCl_n^{(n-1)-}]/[Ag^+][Cl^-]^n$.

TABLE 3: Contents of Amino Acid Residues (A_i) as a Component of Gelatin Responsible for the Formation of Complexes with Ag^+ Ion, pK_a at 25 °C, and the Stability Constants (β) of the Silver Complexes and Their Concentration [Ag − A_i] in a 2 w/v% Gelatin Solution at pCl = 3 and a Temperature of 30 °C

amino acid residue	content (mmol/g)	reactive moiety	pK_a at 25 °C	β at 30 °C	[Ag − A_i] at 30 °C (mol/dm^3)
methionine	0.038	thioether sulfur		$10^{3.11}$	2.35×10^{-7}
histidine	0.041	imidazole group	6.0	$10^{3.29}$	1.42×10^{-7}
lysine	0.267	ϵ-amino group	10.5	$10^{4.44}$	6.58×10^{-10}
glutamic acid	0.703	carboxyl group	4.1	$10^{1.4}$	8.30×10^{-8}
aspartic acid	0.452	carboxyl group	3.9	$10^{1.4}$	5.38×10^{-8}

TABLE 4: Mean Radius of Silver Complexes (r), Viscosity of the Solutions in Reaction (η), Diffusion Coefficient of the Silver Complexes (D), and the Solubility of AgCl Bulk Crystals (C_∞) Used for the Calculation of the Theoretical and Experimental Values of $\dot{v}$[a]

system	r (nm)	η (mPa s)	D (m^2/s)	C_∞ (mol/dm^3)	$\dot{v}$ (nm^3/s) theoretical	$\dot{v}$ (nm^3/s) experimental
AGS system	0.144	2.54	6.07×10^{-10}	1.34×10^{-6}	344	361
RM system	1.63	0.99	1.38×10^{-10}	4.44×10^{-9}	0.259	0.270

[a] For these calculations, $\sigma = 100$ mJ/m^2 and $V_m = 25.78$ cm^3/mol (see eq 3).

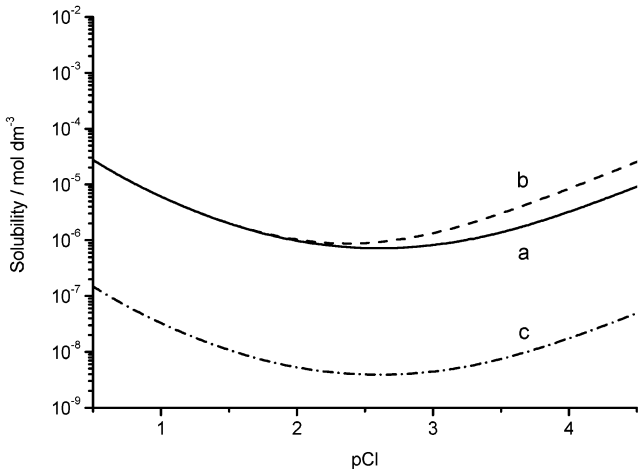

Figure 8. Solubility of bulk AgCl solid, as a function of pCl (≡ −log [Cl$^-$]) in an aqueous solution (curve a, solid line), the aqueous gelatin solution (2 w/v%) (curve b, dashed line), and the reverse micelle (RM) system (Rw = 3) (curve c, dotted-dashed line), at 30 °C.

Figure 8 shows the solubility of AgCl solid in an aqueous solution (Figure 8a), the AGS system (Figure 8b), and the RM system (Figure 8c), as a function of pCl.

Now, we are ready to calculate the diffusion coefficients of Ag-ion complexes (D), from the data of their radius (r) and the viscosity of the medium (η), using eq 5, and calculate the growth rates in volume ($\dot{v}$), from D and the solubility of the AgCl bulk solid (C_∞), using eq 3, for both the AGS and RM systems. The hydrodynamic radius of $AgNO_3$, obtained from its diffusivity,[41] was used for the mean radius of $AgCl_n^{(n-1)-}$ complexes. For the specific surface energy of AgCl (σ), we use the value of 100 mJ/m^2 in the literature.[40] The values of r, η, D, C_∞, and the thus-calculated theoretical $\dot{v}$ for the standard AGS and RM systems are summarized in Table 4, together with the experimental $\dot{v}$ values for the AGS and RM systems obtained from the slopes of the straight lines in Figures 2 and 3, using the general eq 1. The excellent agreement between the theoretical and experimental values of $\dot{v}$ in both AGS and RM systems reconfirms the validity of eq 2 and strongly supports the present model for the formation of AgCl nanoparticles in the RM system.

The fundamental formation mechanism is the same as that in the AGS system, except for the differences in the solubility of the solid and the diffusivity of the Ag-ion complexes; therefore, the dramatic reduction of the particle size in the RM system must be caused by the drastically limited growth rate, which is mainly due to the extremely low solubility of the solid, given by $C_\infty^w V_w/(V_w + V_O)$, and partially due to the small diffusivity of the bulky micellar silver complexes. One may find that this model essentially differs from the conventional view on the particle formation in RM systems, usually explained on the basis of the reactions within the individual reverse micelles, which serve as nanoreactors; this model not only conforms with the fact that each reverse micelle contains only one or no reactant ion or molecule in most RM systems, but it also is consistent with the dynamic and pliable behavior of reverse micelles.

The value of Rw in the RM system in the present study was fixed at 3; therefore, the water in the reverse micelle was expected to be bound, more or less, by NP-6. However, in view of the excellent agreement between the experimental result and the theoretical prediction with the solubility of AgCl bulk solid calculated on the assumption of free water in the reverse micelles, this type of effect on the solubility of AgCl crystals seems negligible.

If the particles are grown by a reaction-controlled mechanism in the present RM system, the general eq 1 may still be valid, but eqs 2 and 3 may not. In this case, the value of $\dot{v}$ in eq 1 is considerably smaller than that in eq 3 for the diffusion-controlled mechanism; thus, much smaller particles are expected to be formed, because of the greater n_∞ value. Although the exceedingly low solubility of the solid in RM systems based on eq 4, which leads to very small particles, is still effective in the reaction-controlled system, the relatively low diffusivity of micellar complexes may have no influence on the particle growth, because the diffusion of the micellar complexes in this case is not the rate-determining step.

If the reactants are introduced instantaneously only in the beginning in the present RM system, the nuclei that are generated first must be grown by ordinary Ostwald ripening, as typically observed in aqueous closed systems.[42,43] Because all the foregoing studies on the particle formation of silver halides in RM systems have been performed using instantaneous mixing and the Ostwald ripening process has never been taken into account, the growth mechanism must be reconsidered from this viewpoint. For example, the effect of Rw (which is defined as [water]/[surfactant]) on the particle size of silver halides grown in RM systems is usually explained in terms of the size of the water pools or the state of water, free or bound, in reverse

micelles.[24,44,45] The same effect, alternatively, may be explained in terms of the solubility of the silver halide crystals in the RM systems, changing with $V_w/(V_w + V_O)$ in eq 4. Also, Hirai et al. proposed a coagulation mechanism for the growth of metal sulfide particles (such as CdS and ZnS[7]) and silver halide particles (such as AgBr and AgI[24]) in the RM systems. Generally, the growth rate of particles is independent of their initial number density in Ostwald ripening, but the growth rate is proportional to the second power of their initial number density in the coagulation process. The data of Hirai et al., reviewed on these criteria, are likely to suggest that the Ostwald ripening process is dominant for ZnS, AgBr, and AgI particles, whereas the contribution of the coagulation process is significant for CdS particles in their system.

The particle size also is dependent on the species of surfactants; for example, Aerosol OT yielded much smaller AgBr particles than NP-6 under the otherwise same conditions in RM systems.[45] Moreover, it is known that the size of the AgBr particles increases as the chain length of alkanes (such as *n*-hexane, *n*-heptane, and *n*-octane) increases; such alkanes are used as a medium of the RM system with Aerosol OT.[44] These effects may suggest a strong interaction between the Aerosol OT and the AgBr particles and alteration of the growth mechanism from diffusion-controlled Ostwald ripening to a reaction-controlled mechanism. The chain length of the alkane media may affect the interaction between the Aerosol OT and the AgBr particles.

Although the Ostwald ripening process may not be ubiquitously observed in all RM systems, the role of reverse micelles as a monomeric solute species in organic media and the dramatic reduction of the substantial solubility of the precipitate seem to be general characteristics of the particle formation in RM systems.

Acknowledgment. The authors would like to thank Lion Co., Ltd., for kindly providing the NP-6 and Prof. K. Kon-No (Tokyo University of Science) for his arrangement. Acknowledgment is also due to Dr. T. Kamiyama (Institute for Materials Research, Tohoku University) for his helpful advice in regard to the SAXS measurements.

References and Notes

(1) Boutonnet, M.; Kizling, J.; Stenius, P.; Maire, G. *Colloids Surf.* **1982**, *5*, 209.
(2) Barnickel, P.; Wokaun, A.; Sager, W.; Eicke, H.-F. *J. Colloid Interface Sci.* **1992**, *148*, 80.
(3) Petit, C.; Lixon, P.; Pileni, M. P. *J. Phys. Chem.* **1993**, *97*, 12974.
(4) Gobe, M.; Kon-No, K.; Kandori, K.; Kitahara, A. *J. Colloid Interface Sci.* **1983**, *93*, 293.
(5) Kawai, T.; Fujino, A.; Kon-No, K. *Colloids Surf. A* **1996**, *109*, 245.
(6) Motte, L.; Petit, C.; Boulanger, L.; Lixon, P.; Pileni, M. P. *Langmuir* **1992**, *8*, 1049.
(7) Hirai, T.; Sato, H.; Komasawa, I. *Ind. Eng. Chem. Res.* **1994**, *33*, 3262.
(8) Monnoyer, Ph.; Fonseca, A.; Nagy, J. B. *Colloids Surf. A* **1995**, *100*, 233.
(9) Dvolaitzky, M.; Ober, R.; Taupin, C.; Anthore, R.; Auvray, X.; Petipas, C.; Williams, C. *J. Dispersion Sci. Technol.* **1983**, *4*, 29.
(10) Chew, C. H.; Gan, L. M.; Shah, D. O. *J. Dispersion Sci. Technol.* **1990**, *11*, 593.
(11) D'Aprano, A.; Pinio, F.; Liveri, V. T. *J. Solution Chem.* **1991**, *20*, 301.
(12) Pillai, V.; Kumar, P.; Hou, M. J.; Ayyub, P.; Shah, D. O. *Adv. Colloid Interface Sci.* **1995**, *55*, 241.
(13) Bagwe, R. P.; Khilar, K. C. *Langmuir* **1997**, *13*, 6432.
(14) Jeunieau, L.; Nagy, J. B. *Colloids Surf. A* **1999**, *151*, 419.
(15) Leong, Y. S.; Candau, F. *J. Phys. Chem.* **1982**, *86*, 2269.
(16) Candau, F.; Leong, Y. S.; Pouyet, G.; Candau, S. *J. Colloid Interface Sci.* **1984**, *101*, 167.
(17) Pileni, M. P. *Langmuir* **1997**, *13*, 3266.
(18) Tanori, J.; Pileni, M. P. *Langmuir* **1997**, *13*, 639.
(19) Fletcher, P. D. I.; Howe, A. M.; Robinson, B. H. *J. Chem. Soc., Faraday Trans. 1* **1987**, *83*, 985.
(20) Tanaka, T.; Iwasaki, M. *J. Photogr. Sci.* **1983**, *31*, 13.
(21) Sugimoto, T. *Monodispersed Particles*; Elsevier: Amsterdam, 2001.
(22) Nagase, K.; Sakaguchi, K. *Kogyo Kagaku Zasshi* **1961**, *64*, 635.
(23) Leubner, I. H. *J. Imaging Sci.* **1985**, *29*, 219.
(24) Sato, H.; Hirai, T.; Komasawa, I. *J. Chem. Eng. Jpn.* **1996**, *29*, 501.
(25) Sugimoto, T. *J. Colloid Interface Sci.* **1992**, *150*, 208.
(26) Berry, C. R. *Photogr. Sci. Eng.* **1976**, *20*, 1.
(27) Akers, R. J.; Riley, P. W. *J. Colloid Interface Sci.* **1974**, *48*, 162.
(28) Sugimoto, T.; Zhou, X.; Muramatsu, A. *J. Colloid Interface Sci.* **2003**, *259*, 53.
(29) Mumaw, C. T.; Haugh, E. F. *J. Imaging Sci.* **1986**, *30*, 198.
(30) Strong, R. W.; Wey, J. S. *Photogr. Sci. Eng.* **1979**, *23*, 344.
(31) Sugimoto, T. *J. Colloid Interface Sci.* **1983**, *93*, 461.
(32) Sugimoto, T. *J. Colloid Interface Sci.* **1983**, *91*, 51.
(33) Sugimoto, T.; Shiba, F.; Sekiguchi, T.; Itoh, H. *Colloids Surf. A* **2000**, *164*, 183.
(34) James, T. H., Ed. *The Theory of the Photographic Process*, 4th ed.; Macmillan Co.: New York, 1977.
(35) Hoyen, H. A., Jr.; Cole, R. M. *J. Colloid Interface Sci.* **1972**, *41*, 93.
(36) Clark, R. C.; Courts, A. *The Science and Technology of Gelatin*; Academic Press: London, 1977; p 211.
(37) Russel, G. *J. Photogr. Sci.* **1967**, *15*, 151.
(38) Ooki, M. et al., Eds., *Kagaku Jiten*; Tokyo Kagaku Dojin Co.: Tokyo, 1994.
(39) Harding, M. J. *J. Photogr. Sci.* **1979**, *27*, 1.
(40) Sugimoto, T.; Shiba, F. *J. Phys. Chem. B* **1999**, *103*, 3616.
(41) *Kagaku Binran*, revised 4th ed.; Chemical Society of Japan and Maruzen Co.: Tokyo, 1993.
(42) Sugimoto, T.; Yamaguchi, G. *J. Phys. Chem.* **1976**, *80*, 1579.
(43) Sugimoto, T. *Photogr. Sci. Eng.* **1984**, *28*, 137.
(44) Johansson K. P.; Marchetti, A. P.; McLendon, G. L. *J. Phys. Chem.* **1992**, *96*, 2873.
(45) Kon-no, K. In *Fine Particles: Synthesis, Characterization, and Mechanisms of Growth*, Sugimoto, T., Ed.; Marcel Dekker: New York, 2000; p 302.